Electric Vehicle Charging with Multi-Port Converter based Integration in DC Trolley-Bus Network

Shekhar, Aditya; Chandra Mouli, Gautham Ram; Bandyopadhyay, Soumya; Bauer, Pavol

DOI
10.1109/PEMC48073.2021.9432590

Publication date
2021

Document Version
Final published version

Published in
Proceedings - 2021 IEEE 19th International Power Electronics and Motion Control Conference, PEMC 2021

Electric Vehicle Charging with Multi-Port Converter based Integration in DC Trolley-Bus Network

Aditya Shekhar, Gautham Chandra Ram Mouli, Soumya Bandyopadhyay and Pavol Bauer

2021 IEEE 19th International Power Electronics and Motion Control Conference (PEMC) | 978-1-7281-5660-6/20/$31.00 ©2021 IEEE | DOI: 10.1109/PEMC48073.2021.9432590

***Abstract*—DC traction networks that supply power to trolley-buses, tramcars and trains can be simultaneously used to integrate fast-charging stations for Electric Vehicles (EVs). This strategy improves the traction grid utilization of urban transportation systems. In addition, it offers a potential solution to the increasing requirement of charging infrastructure due to proliferation of plug-in EVs and the associated impact on the existing distribution network. This paper suggests that the use of multi-port converter based integration of EV chargers with dc trolley-bus network can be a preferred solution in terms of defined efficiency boundary. A sensitivity analysis to charging power, substation distance and section length of overhead contact system is performed in comparison to the conventional two-port dc/dc converter based EV integration.**

***Index Terms*—bilateral connection, electric vehicles, dc fast charging, subway, traction systems, tramway network, transportation electrification, triple-active bridge, wayside storage.**

I. Introduction

Electric Vehicles (EVs) will become the preferred mode of transport in future. Uncontrolled plug-and-charge of the on-board batteries of these EVs can increase the peak power demand on the existing distribution networks. For example, [1] suggests that 60 % EV penetration can lead to overloads in local distribution networks in Hungary, while [2] shows that significant transformer overloads in the range of 125-180 % can be expected in Dutch sub-urban distribution grids with 20-80 % EV penetration. As a consequence, the grid infrastructure must be reinforced to supply the higher demand. In this context, the use of dc in restructuring existing distribution networks for capacity enhancement is relevant [3]–[5]. This paper proposes to charge electric vehicles from dc traction systems, specifically but not limited to trolley grids, using multi-port converters.

Present dc traction power systems are dedicated to dynamically supply power to public transport vehicles such as trolley-buses, tram cars and trains. The capacity of these systems are typically designed to power the peak demand of a specified number of connected vehicles during acceleration. The infrastructure is under-utilized because such events are less frequent and of low duration. Furthermore, these supply systems are typically oversized, keeping in mind the future requirements due to load growth. A recent study [6] for trolley-bus system in Poland recommends that cities already operating such systems should consider utilizing the infrastructure for In-Motion Charging (IMC) with trade-off for investment cost and battery capacity.

Fig. 1: Stationary EV charging by co-utilizing the trolley-bus network [10].

In [7], it is suggested that the trolley-bus catenary grid in Solingen, Germany can be simultaneously used for stationary EV charging. The study suggests the use of smart EV charging strategy to account for the fluctuations in available power capacity due to operating trolley-buses on the sections. Similar applications of co-utilizing traction grids for charging purposes is offered in [8], [9]. For example, [8] suggests that by exploiting the tramway and trolleybus infrastructure for charging of electric buses, installation of additional lines to the charging points from the public distribution grid can be avoided, thus reducing costs and construction process. Furthermore, the traction network is dc, unlike the medium voltage ac distribution grid, which can reduce losses and costs of conversion associated particularly with fast EV charging application. A recent demonstration pilot site for stationary EV charging by co-utilizing the trolley-bus network is planned in The Netherlands, as shown in Fig. 1.

The focus of this paper is to determine the efficiency boundaries of the multi-port converter based EV integration using the example of dc trolley-bus networks. The concept can also be applied to other structurally similar traction supply systems. Fig. 2 illustrates a trolley-bus grid in which the overhead conductors are simultaneously used to charge Electric Vehicles (EVs). Two different types of integration strategies are shown using two-port converter (2PC) and three-port converter (3PC).

The authors are with the Department of Electrical Sustainable Energy in the DCE&S Group, Delft University of Technology, The Netherlands. Email: a.shekhar@tudelft.nl, p.bauer@tudelft.nl. This study is funded by the Trolley 2.0 project https://www.trolleymotion.eu/trolley2-0/.

978-1-7281-5660-6/21/$31.00 ©2021 IEEE

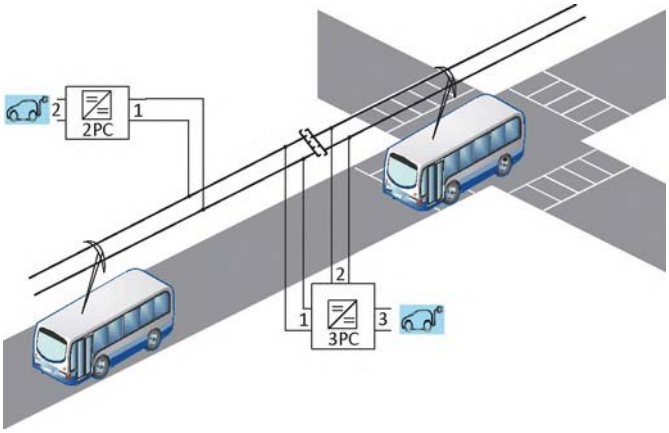

Fig. 2: Illustration of MPC based integration of EV chargers with dc trolley-bus networks.

The main difference between the two schemes is that the 2PC draws charging power from a single trolley-grid section while 3PC is connected to two consecutive electrically isolated overhead sections. As a consequence the load current associated with the latter is split according to the power drawn by port 1 and port 2 of the 3PC. The contributions of this paper are the following:

- Determine the critical length ($L_{\max}$) of the overhead trolley grid section below which 3PC is more efficient than 2PC based integration of EV charger.
- Perform sensitivity analysis to show variation in $L_{\max}$ with substation distance from the trolley sections, charging power and the converter efficiency.

II. System Description

A. Equivalent Circuit

Fig. 3a and Fig. 3b shows the equivalent circuit for the 2PC (with efficiency η_{2pc}) and 3PC (with efficiency η_{3pc}) based integration of EV charging with the trolley grid sections, respectively.

In this system v_s is the dc output voltage of the rectifier based substation that supplies power to several electrically isolated overhead conductors of the trolley-bus network. Two consecutive sections of lengths l_{sec} and $k_{sec}l_{sec}$ are considered, where k_{sec} is the ratio of the lengths of these sections. The substation feeders are at a distance of l_s and $k_s l_s$, with k_s being the ratio of the substation distance from the two sections. Typically, the substation distance from the overhead sections is upto 5 km for centrally located rectifiers and 1-3 km for decentralized systems [20]. The choice of spatial structure of the traction grid has significant impact on the transmission losses of the system. r_s is the resistance in Ω/km for the underground cable circuit that connects the dc substation to the overhead sections. In the equivalent circuit, connection points x and x' indicate the location at which the underground cable system is connected to the overhead line conductors of the corresponding sections. r_{sec} is the resistance in Ω/km for the overhead section circuit. P_{ev} is the EV charging power drawn from the trolley grid network.

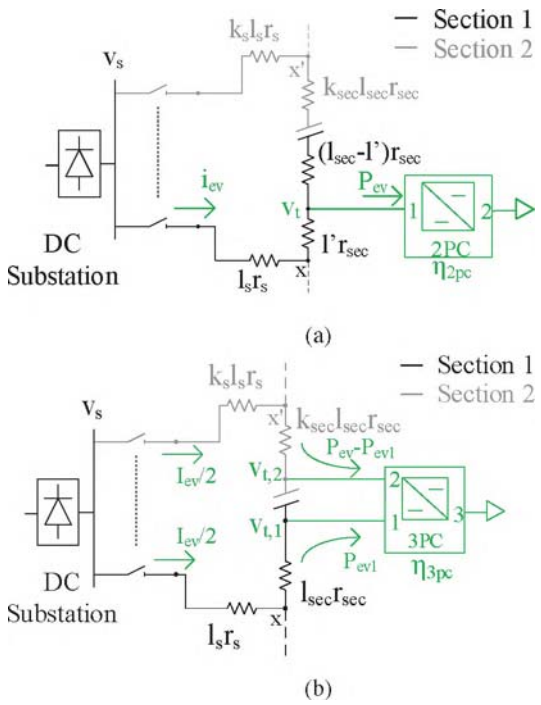

Fig. 3: Equivalent circuit for EV charger integrated with dc trolley grid section using (a) 2-port dc/dc converter (b) 3-port dc/dc converter.

Fig. 3a shows that the 2PC based EV charger is connected l' distance away from x. While l' can be freely chosen, l'=0 gives minimum network conduction losses for 2PC based EV integration. v_t is the terminal voltage at the point of coupling between the port 1 of the 2PC and the overhead section. The corresponding EV charging current drawn is given by (1).

$$i_{ev} = \frac{P_{ev}}{v_t} \tag{1}$$

In case of 3PC (Fig. 3b), the two input ports (1 and 2) draw half the charging power P_{ev} each, through terminal voltages $v_{t,1}$ and $v_{t,2}$ respectively. For a generic case, the the total power can be shared in any proportion between the two sections. The location of 3PC is fixed at the end points of the two consecutive overhead sections and cannot be freely chosen. As a consequence, the input ports 1 and 2 of the 3PC are l_{sec} and $k_{sec}l_{sec}$ away from points x and x' respectively. As the distance between points x and x' ($l_{sec}(1+k_{sec})$) increases, the operating losses with 3PC based EV charging increase. However, because the drawn charging current is split between two parallel paths in the network, the system efficiency can be higher than 2PC based integration depending on the system parameters. In this paper the efficiency boundary $(l_{sec}(1+k_{sec})) \leq l_{max}$ will be defined for which 3PC is a more efficient solution as compared to 2PC for EV integration with the trolley network. Sensitivity analysis will be performed to determine the variation in l_{max} for varying system parameters like rated EV charging power P_{ev}, substation distance l_s, ratio k_s and difference in converter efficiencies $\Delta\eta = \eta_{3pc} - \eta_{2pc}$.

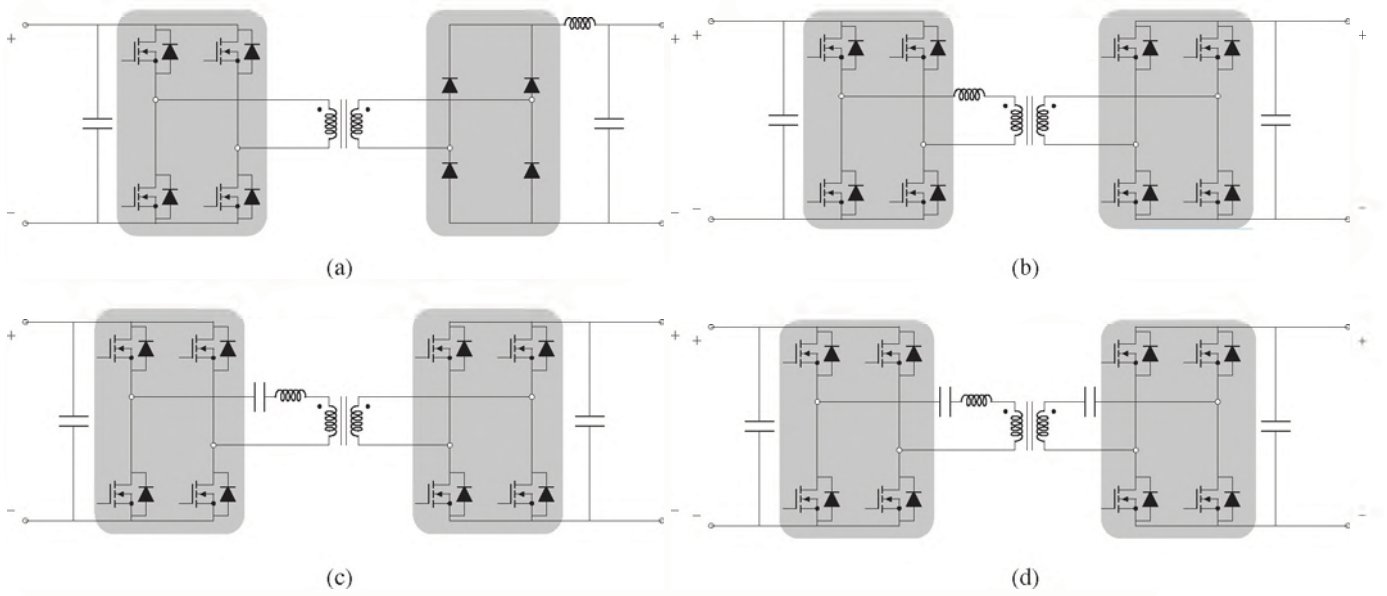

Fig. 4: Isolated dc–dc converter topologies for dc fast chargers, : (a) PSFB converter, (b) DAB converter, (c) LLC converter, and (d) CLLC converter.

TABLE I: Comparison of isolated DC-DC converter topologies for EV charging

Converter topology	Bi-directional	Advantages	Disadvantages	Literature
PSFB	No	Simple control Wide output range	High switching losses Low ZVS range	[11], [12]
DAB	Yes	Simple control Wide output range	Trade-off between reactive power and ZVS range	[13]–[15]
LLC	Yes	Low reactive current ZVS in primary ZCS in secondary	Limited controllability Low ZVS range	[16], [17]
CLLC	Yes	Low reactive current Wide ZVS range	Limited controllability	[18], [19]

B. Converter Topologies

A dc-dc converter is used to provide an interface between the DC trolley grid and the EV battery. Isolated converter topologies are considered for EV charging application in this paper to ensure galvanic isolation between the grid and the battery. Fig. 4 shows four popular isolated dc-dc converter topologies reported in literature. Phase-Shifted Full Bridge (PSFB) and Dual Active Bridge (DAB) topology is considered. The operational advantages and disadvantages as well as associated references are listed in Table I.

Multi-port converters (MPC) have become a widely-researched candidate for the integration of multiple renewable sources, storage and loads [21]. The topology of MPC is shown in Fig. 5. Connecting multiple ports reduces power conversion stress, improves efficiency, reduces material billing and increases power density. Therefore, multi-port converters have many potential applications: (1) more electric aircraft or all-electric ship [22]–[24], (2) electric vehicle (EV) charging applications [25]–[27], (3) energy router for smart homes [28], (4) solid-state transformer (SST) cross-link between medium voltage (MV) and low voltage grid (LV). The main advantage of the MPC is it's capability to integrate multiple ports with varied voltage and current ratings into a single power stage allowing bi-directional power flow between each port. 750 V DC EV charging integrated with solar generation is explored in [29], [30]. With the advent of such applications for EV chargers, PV systems, and storage, MPC converters can also have a huge potential in single-hub integration of these systems.

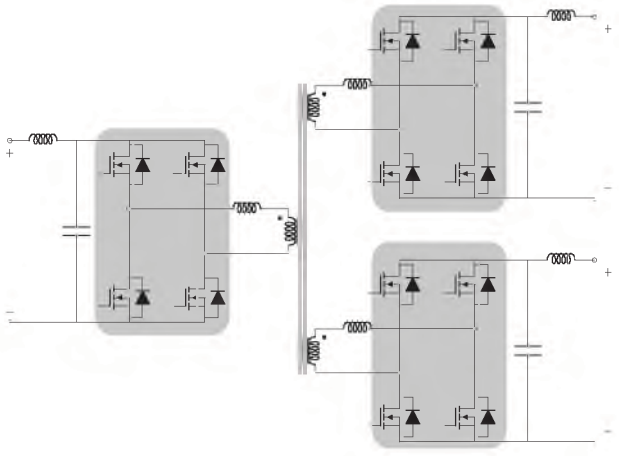

Fig. 5: Isolated triple-active bridge (TAB) converter topology

III. Efficiency Boundary for Integration with Multi-port Converter

A. Losses with 2PC based integration

The input terminal voltage of the EV charger (v_t) is given by (2).

$$v_t = v_s - i_{ev}(l_s r_s + l' r_{sec}) \tag{2}$$

Equations (1) and (2) can be iteratively solved with the initial value of v_t corresponding to the output dc voltage of the rectifier substation (v_s). Herein, l' is the distance of the point of EV integration from the substation connection point x at the trolley section and can be freely chosen with the system losses ($P_{loss,2pc}$) given by (3).

$$P_{loss,2pc} = P_{ev}(1 - \eta_{2pc}) + i_{ev}^2(l_s r_s + l' r_{sec}) \tag{3}$$

It can be inferred that the minimum losses with 2PC based integration ($P_{l,2pc,min} = \min(P_{loss,2pc})$) occurring at $l' = 0$.

B. Losses with 3PC based integration

Each input port of the 3PC supplies a part of the EV charging power as described by (4).

$$P_{ev} = P_{ev,1} + P_{ev,2} \tag{4}$$

The corresponding currents drawn from each section can be estimated using (1).

$$i_{ev,3pc,1} = \frac{P_{ev,1}}{v_{t,1}} \tag{5}$$

$$i_{ev,3pc,2} = \frac{P_{ev,2}}{v_{t,2}} \tag{6}$$

The terminal voltages $v_{t,1}$ and $v_{t,2}$ are given by (7) and (8) respectively.

$$v_{t,1} = v_s - i_{ev,3pc,1}(l_s r_s + l_{sec} r_{sec}) \tag{7}$$

$$v_{t,2} = v_s - i_{ev,3pc,2}(k_s l_s r_s + k_{sec} l_{sec} r_{sec}) \tag{8}$$

The system loss with 3PC based EV integration ($P_{loss,m=3pc}$) is given by (9).

$$P_{loss,3pc} = P_{ev}(1 - \eta_{3pc}) + i_{ev,3pc,1}^2(l_{sec} r_{sec} + l_s r_s) + i_{ev,3pc,2}^2(k_{sec} l_{sec} r_{sec} + k_s l_s r_s) \tag{9}$$

C. Sensitivity Analysis with EV Charging Power Level

Length $l_{xx'}$ is defined in (10) as the distance between the two substation connections x and x' of the consecutive sections.

$$l_{xx'} = l_{sec}(1 + k_{sec}) \leq l_{xx',max} \tag{10}$$

Let $l_{xx',max}$ be the boundary such that for all $l_{xx'} \leq l_{xx',max}$, 3PC based EV integration is more efficient than that with 2PC. The value of $l_{xx',max}$ can be determined by equating $P_{loss,2pc} = P_{loss,3pc}$ from (3) and (9). Fig. 14 shows the variation in $l_{xx',max}$ for varying EV charging powers and converter efficiency difference $\Delta\eta = \eta_{3pc} - \eta_{2pc}$ for two different substation distances.

The results are plotted with the following assumptions:

- The substation distances from x and x' are equal ($k_s = 1$).
- The ratio of the two consecutive sections is equal ($k_{sec} = 1$).
- The power drawn by the two input ports of the 3PC are equal and half of the total EV charging power ($P_{ev,1} = P_{ev,2} = P_{ev}$).
- The 2PC is connected at $l' = 0$, giving minimum possible $P_{loss,2pc}$ for the considered operating conditions ($P_{l,2pc,min}$).

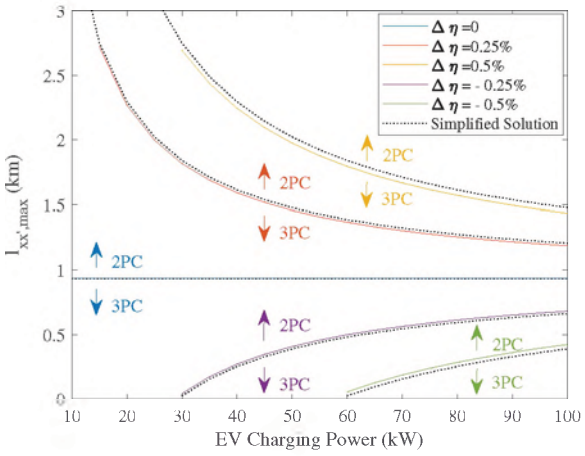

(a)

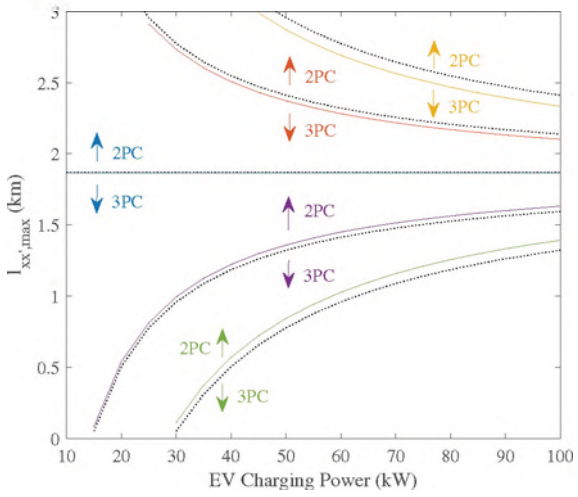

(b)

Fig. 6: Maximum section length with varying EV charging power for different $\Delta\eta$ with (a) l_s=1 km (b) l_s=2 km.

It can be observed that as the distance of the substation l_s increases from 1 km in Fig. 6a to 2 km in Fig. 6b, $l_{xx',max}$ increases implying larger boundary within which 3PC based EV integration solution is more efficient. This boundary is independent of P_{ev} if the considered converters have the same efficiency ($\Delta\eta = 0$). For the given P_{ev}, $l_{xx',max}$ increases with increasing $\Delta\eta$ as a consequence of reduction in converter losses with 3PC as compared to 2PC. If MPC is less efficient than the two-port converter ($\Delta\eta < 0$), the $l_{xx',max}$ increases with P_{ev} and vice versa if $\Delta\eta > 0$.

D. Simplified Solution for $l_{xx',max}$

While the plotted results are determined by iteratively solving the loss equations based on the given operating conditions, the dotted lines in Fig. 6 show the solution for $l_{xx',max}$ using a derived expression based on the simplifying assumption that the terminal voltage at the input side of the converter is equal to the substation voltage ($v_t = v_{t,1} = v_{t,2} = v_s$). This can be a reasonable assumption because the system conductors are sized for sufficient power capability and small voltage drops at these power levels. It will be shown that the losses and corresponding efficiency boundaries do not deviate significantly with this assumption. Therefore, the EV charging current drawn from the trolley grid is given by (11).

$$i_{ev} = \frac{P_{ev}}{v_s} \tag{11}$$

As a result, the simplified loss powers $P_{l,2pc,min}$ and $P_{l,3pc}$ are given by (12) and (13), respectively.

$$P_{l,2pc,min} = (1-\eta_{2pc})P_{ev} + \left(\frac{P_{ev}}{v_s}\right)^2 l_s r_s \tag{12}$$

$$P_{l,3pc} = (1-\eta_{3pc})P_{ev} + \left(\frac{P_{ev}}{v_s}\right)^2 \left(\frac{r_{sec} l_{sec}(1+k_{sec}) + r_s l_s (1+k_s)}{4}\right) \tag{13}$$

Equating (12) and (13) and rearranging, the boundary $l_{sec,max}$ can be determined with (14).

$$l_{xx',max} = \left(\frac{v_s^2}{P_{ev}}(\eta_{3pc}-\eta_{2pc}) + l_s r_s \left(\frac{3-k_s}{4}\right)\right)\frac{4}{r_{sec}} \tag{14}$$

It can be observed from the dotted lines in Fig. 6 that the simplified solution is close to the exact solution. The advantage of (14) is that the tendencies in variation of the efficiency boundary of 3PC based integration with variation in different operating parameters can be estimated with reasonable accuracy.

E. Substation distance from Trolley Grid Sections

Fig. 7 shows the variation in $l_{xx',max}$ with substation distance l_s for different k_s considering $\Delta\eta = 0$.

It can be observed that for the given l_s, $l_{xx',max}$ decreases with increasing k_s until a maximum of $k_s = 3$. This indicates that 3PC can be more efficient for a given system even when the connection point x' of the subsequent trolley section is location 3 times further away from the feeding substation as compared to the location of x.

IV. Other Trade-offs and Considerations

A. Flexibility of Location

In the discussion thus far, $l' = 0$ is assumed to determine the efficiency boundary $l_{xx',max}$ corresponding to $P_{l,2PC,min}$. It can be inferred that $l_{xx',max}$ will linearly increase with increasing $l' > 0$ as a consequence of increase in losses for the 2PC based integration given by (15).

$$l_{xx',max} = l_{xx',max}(l'=0) + 4l' \tag{15}$$

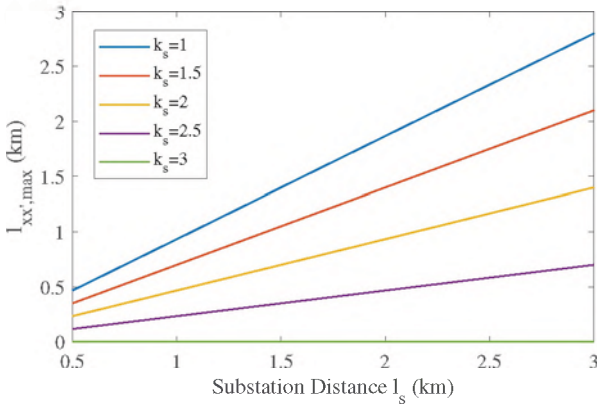

Fig. 7: $l_{xx',max}$ as a function of substation distance l_s for different k_s.

Therefore, the location of 2PC at $l' > 0$ increases the efficiency boundary for which the 3PC based EV integration method is preferred. However, the flexibility of choosing the location of EV charger on the trolley grid section can be an important advantage from practical system design standpoint, even if it comes at the cost of lower operating efficiency.

B. Capacity Footprint

The focus of this paper is to simultaneously use the trolley grid infrastructure for stationary EV charging application. The concept is based on the understanding that the trolley-bus supply system is currently underutilized, depending on the schedule and traffic conditions over the day. For example, the maximum power demand on a particular grid section depends on the accelerating trolley-buses connected to it. The system is designed to handle such events though these are of relatively low duration and frequency and thus the grid capacity is underutilized because the supply is presently dedicated only to power trolley-buses.

When using the same infrastructure for stationary EV charging, its capacity footprint on the trolley grid in terms of both operating current and voltage dip is important. For the given charging power, the operating current gets split to two sections in case of 3PC based integration. Consequently, its capacity footprint in terms of magnitude is lower as compared to the 2PC based integration. However, as a trade-off, the impacted region of the trolley grid is higher for 3PC. Specifically, the current-carrying capacity of the segmented overhead section between x-x' in Fig. 3b is lower than the underground cables between the substations and these locations. Since 3PC-based EV integration inevitably loads a greater part of this region of the grid as compared to 2PC, the associated loading factor as a percentage of capacity can be higher, albeit at lower current magnitude for the same charging power. In other words, if l' =0 is chosen for 2PC, the loading of the overhead section, which is usually the limiting region of the system, is avoided and can be a preferred solution in terms of capacity footprint even though the current flowing in the grid is higher than the 3PC based charging.

As highlighted, the accelerating trolley-buses can be considered as a short-duration transient loads on the grid sections. Therefore, smart EV charging solutions that prioritize these events can improve the utilization.

V. Conclusions

It is important to consider that dc traction supply systems of urban transportation networks are typically under-utilized. This paper suggested that the infrastructure can simultaneously used for stationary charging of EVs.

The main conclusion is that system efficiency can be higher with multi-port converter based integration of EV chargers as compared to two-port converter. The sensitivity analysis on the described efficiency boundary shows that preference of MPC increases with substation distance and EV charging power. Furthermore, it is discussed that the capacity footprint of MPC based integration can be lower but some drawbacks related to flexibility of location and impacted grid region are highlighted.

References

[1] H. Ramadan, A. Ali, and C. Farkas, "Assessment of plug-in electric vehicles charging impacts on residential low voltage distribution grid in hungary," in *2018 6th International Istanbul Smart Grids and Cities Congress and Fair (ICSG)*, 2018, pp. 105–109.

[2] Y. Yu, A. Shekhar, G. C. R. Mouli, P. Bauer, N. Refa, and R. Bernards, "Impact of uncontrolled charging with mass deployment of electric vehicles on low voltage distribution networks," in *2020 IEEE Transportation Electrification Conference Expo (ITEC)*, 2020, pp. 766–772.

[3] G. Jambrich, J. Stöckl, and M. Makoschitz, "Mvdc ring-cable approach for new dc distribution and restructured ac grids," in *2019 IEEE Third International Conference on DC Microgrids (ICDCM)*, 2019, pp. 1–5.

[4] A. Shekhar, E. Kontos, L. Ramirez-Elizondo, A. Rodrigo-Mor, and P. Bauer, "Grid capacity and efficiency enhancement by operating medium voltage ac cables as dc links with modular multilevel converters," *International Journal of Electrical Power & Energy Systems*, vol. 93, pp. 479–493, 2017.

[5] A. Shekhar, L. Ramírez-Elizondo, X. Feng, E. Kontos, and P. Bauer, "Reconfigurable dc links for restructuring existing medium voltage ac distribution grids," *Electric Power Components and Systems*, vol. 45, no. 16, pp. 1739–1746, 2017.

[6] M. Wołek, M. Wolański, M. Bartłomiejczyk, O. Wyszomirski, K. Grzelec, and K. Hebel, "Ensuring sustainable development of urban public transport: A case study of the trolleybus system in gdynia and sopot (poland)," *Journal of Cleaner Production*, vol. 279, p. 123807, 2021. [Online]. Available: http://www.sciencedirect.com/science/article/pii/S095965262033852X

[7] M. Weisbach, U. Spaeth, B. Schmuelling, and C. Troullier, "Flexible ev charging strategy for a dc catenary grid," in *2020 Fifteenth International Conference on Ecological Vehicles and Renewable Energies (EVER)*, 2020, pp. 1–6.

[8] M. Bartłomiejczyk, "Smart grid technologies in electric power supply systems of public transport," *Transport*, vol. 33, no. 5, pp. 1144–54, 2018.

[9] M. Meng, M. Guo, Y. Yuan, L. Jiang, J. Liu, D. Hu, H. Cong, and D. Hao, "Dc micro-grid based on dc traction power supply system and electric vehicle batteries charging discharging system," in *2014 17th International Conference on Electrical Machines and Systems (ICEMS)*, Oct 2014, pp. 2579–2582.

[10] "https://venematech.nl/wp-content/uploads/2018/03/Eindresultaat4.jpeg," Accessed: March 2020.

[11] J.-G. Cho, J.-W. Baek, C.-Y. Jeong, and G.-H. Rim, "Novel zero-voltage and zero-current-switching full-bridge pwm converter using a simple auxiliary circuit," *IEEE Transactions on Industry applications*, vol. 35, no. 1, pp. 15–20, 1999.

[12] J. Sabate, V. Vlatkovic, R. Ridley, and F. Lee, "High-voltage, high-power, zvs, full-bridge pwm converter employing an active snubber," in *[Proceedings] APEC'91: Sixth Annual Applied Power Electronics Conference and Exhibition.* IEEE, 1991, pp. 158–163.

[13] R. W. De Doncker, D. M. Divan, and M. H. Kheraluwala, "A three-phase soft-switched high-power-density dc/dc converter for high-power applications," *IEEE transactions on industry applications*, vol. 27, no. 1, pp. 63–73, 1991.

[14] G. Oggier, G. O. Garcia, and A. R. Oliva, "Modulation strategy to operate the dual active bridge dc-dc converter under soft switching in the whole operating range," *IEEE Transactions on Power Electronics*, vol. 26, no. 4, pp. 1228–1236, 2010.

[15] F. Krismer and J. W. Kolar, "Efficiency-optimized high-current dual active bridge converter for automotive applications," *IEEE Transactions on Industrial Electronics*, vol. 59, no. 7, pp. 2745–2760, 2011.

[16] B. Yang, F. C. Lee, A. Zhang, and G. Huang, "Llc resonant converter for front end dc/dc conversion," in *APEC. Seventeenth Annual IEEE Applied Power Electronics Conference and Exposition (Cat. No. 02CH37335)*, vol. 2. IEEE, 2002, pp. 1108–1112.

[17] J. E. Huber, J. Miniböck, and J. W. Kolar, "Generic derivation of dynamic model for half-cycle dcm series resonant converters," *IEEE Transactions on Power Electronics*, vol. 33, no. 1, pp. 4–7, 2017.

[18] W. Chen, P. Rong, and Z. Lu, "Snubberless bidirectional dc–dc converter with new cllc resonant tank featuring minimized switching loss," *IEEE Transactions on industrial electronics*, vol. 57, no. 9, pp. 3075–3086, 2009.

[19] Z. U. Zahid, Z. M. Dalala, R. Chen, B. Chen, and J.-S. Lai, "Design of bidirectional dc–dc resonant converter for vehicle-to-grid (v2g) applications," *IEEE Transactions on Transportation Electrification*, vol. 1, no. 3, pp. 232–244, 2015.

[20] M. Bartłomiejczyk and M. Połom, "The impact of the overhead line's power supply system spatial differentiation on the energy consumption of trolleybus transport: planning and economic aspects," *Transport*, vol. 32, no. 1, pp. 1–12, 2017. [Online]. Available: https://doi.org/10.3846/16484142.2015.1101611

[21] A. K. Bhattacharjee, N. Kutkut, and I. Batarseh, "Review of multiport converters for solar and energy storage integration," *IEEE Transactions on Power Electronics*, vol. 34, no. 2, pp. 1431–1445, 2018.

[22] P. Wheeler and S. Bozhko, "The more electric aircraft: Technology and challenges." *IEEE Electrification Magazine*, vol. 2, pp. 6–12, 2014.

[23] G. Sulligoi, A. Vicenzutti, and R. Menis, "All-electric ship design: From electrical propulsion to integrated electrical and electronic power systems," *IEEE Transactions on Transportation Electrification*, vol. 2, no. 4, pp. 507–521, 2016.

[24] G. Buticchi, L. F. Costa, D. Barater, M. Liserre, and E. D. Amarillo, "A quadruple active bridge converter for the storage integration on the more electric aircraft," *IEEE Transactions on Power Electronics*, vol. 33, no. 9, pp. 8174–8186, 2017.

[25] H. Chen, Z. Hu, H. Luo, J. Qin, R. Rajagopal, and H. Zhang, "Design and planning of a multiple-charger multiple-port charging system for pev charging station," *IEEE Transactions on Smart Grid*, 2017.

[26] M. Vasiladiotis and A. Rufer, "A modular multiport power electronic transformer with integrated split battery energy storage for versatile ultrafast ev charging stations," *IEEE Transactions on Industrial Electronics*, vol. 62, no. 5, pp. 3213–3222, 2014.

[27] J. Schäfer, D. Bortis, and J. W. Kolar, "Multi-port multi-cell dc/dc converter topology for electric vehicle's power distribution networks," in *2017 IEEE 18th Workshop on Control and Modeling for Power Electronics (COMPEL).* IEEE, 2017, pp. 1–9.

[28] S. Falcones, R. Ayyanar, and X. Mao, "A dc–dc multiport-converter-based solid-state transformer integrating distributed generation and storage," *IEEE Transactions on Power electronics*, vol. 28, no. 5, pp. 2192–2203, 2012.

[29] A. Bassa de los Mozos, G. R. Chandra Mouli, and P. Bauer, "Evaluation of topologies for a solar powered bidirectional electric vehicle charger," *IET Power Electronics*, vol. 12, no. 14, pp. 3675–3687, 2019.

[30] G. R. Chandra Mouli, J. Schijffelen, M. van den Heuvel, M. Kardolus, and P. Bauer, "A 10 kw solar-powered bidirectional ev charger compatible with chademo and combo," *IEEE Transactions on Power Electronics*, vol. 34, no. 2, pp. 1082–1098, Feb 2019.